



ELSEVIER

Contents lists available at ScienceDirect

Polymer Testing

journal homepage: www.elsevier.com/locate/polytestPOLYMER
TESTING

ROGER BROWN

Property Modelling

Parametric study of crushing parameters and failure patterns of pultruded composite tubes using cohesive elements and seam: Part II – Multiple delaminations and initial geometric imperfections

Sivakumar Palanivelu^{a,*}, Wim Van Paepegem^a, Joris Degrieck^a, Johan Van Ackeren^b,
Dimitrios Kakogiannis^b, Jan Wastiels^b, Danny Van Hemelrijck^b, John Vantomme^c

^a Department of Materials Science and Engineering, Ghent University, Sint-Pietersnieuwstraat 41, 9000 Gent, Belgium

^b Department of Mechanics of Materials and Constructions, Vrije Universiteit Brussel, Pleinlaan 2 B-1050 Brussels, Belgium

^c Royal Military Academy, Civil and Materials Engineering Department, Building G, Level 0, 8 Av. Hobbema B-1000, Brussels, Belgium

ARTICLE INFO

Article history:

Received 20 May 2010

Accepted 8 July 2010

Keywords:

Energy absorption

Peak crushing load

Multiple delamination

pre-defined seams

Initial geometric imperfection

ABSTRACT

Part I presented the circumferential central delamination and triggering modelling of composite tubes and their influence on predicting the peak crush load and the corresponding energy absorption. The knowledge of failure patterns is very important for the design architecture of an energy absorbing element and its placement in the structure. In this study, the failure patterns of pultruded circular and square cross sectional glass polyester composite tubes were evaluated with pre-defined seams for an axial impact loading case. Furthermore, this paper demonstrates the importance of considering multiple delaminations to predict the appropriate energy absorption of composite tubes using cohesive elements. The influence of correct numerical modelling of triggering (especially 45° edge chamfering) on the peak crush load of the composite tubes is proved with multiple layers of shell elements. The effect of initial geometric imperfections on the energy absorption, peak crushing load and the deformation pattern of pultruded glass polyester composite tubes is also studied. In order to address the importance of above factors, a comprehensive numerical investigation was carried out with multiple layers of shell elements and with cohesive elements. Finally, the deformation patterns, peak crushing load and the corresponding energy absorption were compared with experimental results [1].

© 2010 Elsevier Ltd. All rights reserved.

1. Introduction

Crashworthy efficient structures must be able to dissipate large amounts of energy in the event of a crash. From the success stories in the aerospace industry, it is widely accepted that polymer composite materials offer a number of technical advantages. Some of them are high specific mechanical properties such as stiffness and strength,

design flexibility, reduced weight and less maintenance. Due to the above factors, in recent times the interest in composite materials has been much increased in the area of impact and blast loading applications [2]. One of the main reasons for this is the higher specific energy absorption of composites over metals and alloys. Few researchers have studied the numerical energy absorption of polymer composite materials for an axial impact event [3–5]. The accuracy of numerical predictions depends upon the correct modelling of the structural geometry, integrating the right damage mechanisms and the accurate modelling of the physics of impact. Part I of this paper dealt with the finite element modelling issues of triggering, especially the

* Corresponding author. Tel.: +32 (0)9 264 33.15; fax: +32 (0)9 264 35 87.
E-mail address: Sivakumar.Palanivelu@UGent.be (S. Palanivelu).

triggering type 1 (45° chamfering) with a single and two layers of shell elements approach to predict the correct peak crush load and the corresponding energy absorption. Furthermore, it was also proved that the incorrect prediction of the peak crush load of a composite tube will provide an unrealistic deformation length and energy absorption. Hence, the correct and accurate modelling of triggering which initiates the initial damage is very important. This paper demonstrates the correct finite element modelling of triggering using multiple layers of shell elements. In order to validate this approach, the numerical peak crush loads of circular and square pultruded glass-polyester composite tubes were compared with experimental data [1].

During an axial impact event, the compressive strength of a composite material will reduce significantly due to delamination. The reduction in compressive strength of composite laminates has been well studied numerically considering structural instability and delamination growth in [6,7]. The influence of delamination failure on concave cylindrical composite test specimens during an impact event using a continuum damage model was studied in [8]. However, the approach of delamination was not previously considered to predict the energy absorption for circular and square composite tubes. Furthermore, the actual deformation of a typical brittle composite tube exhibits multiple delaminations [1,7,9–11]. The consideration of multiple delaminations approach is important because it causes ply separation and loss in bending and compressive stiffness of each sub-laminate [7]. To understand the importance of multiple delaminations on the energy absorption, and to achieve the typical failure patterns of a brittle composite tube, a numerical parametric study was conducted with multiple layers of shell elements and solid cohesive elements.

The approach of two layers of shell elements with cohesive elements provided comparable peak and mean crush loads, deformation length and the corresponding energy absorption for the circular and square composite tubes with triggering type 2 (CP2 and SP2). However, due to the absence of axial cracks, the final deformation patterns were different from experimental results. Hence, an initial evaluation was made to study the effect of axial cracks on the deformation pattern of circular and square composite tubes for Case 2 (Two layers of shell elements with cohesive elements) of Part I. The axial cracks were modelled with pre-defined seams and, further, it was extended to complex models such as multiple layers of shell elements with cohesive elements. Moreover, the effect of the number of pre-defined seams on the peak crushing load and the corresponding energy absorption of the composite tube series was also evaluated.

Studies on composite shells [12–15] have proved that traditional (geometric tube-wall mid-surface imperfections) and non-traditional imperfections (tube wall thickness variation, local tube wall ply gaps, tube end geometric imperfections, non-uniform loading of tubes and variations in the boundary condition) have a large influence on the performance of composite shell structures. Non-traditional imperfections such as variation in the boundary condition and loading can be avoided with proper care during experimental testing. However, the

initial imperfection caused during a manufacturing process, such as variation in material properties at different locations of a composite structure and a variation in structural dimensions, cannot be avoided during an experimental test. Hence, during an analytical study or a finite element calculation it is advisable to consider the above effects to predict the correct performance parameters of a composite structure. Of the mentioned initial imperfections, the influence of initial geometric imperfections on the performance of a composite structure is greatest [12,16,17]. As discussed in Part I, the numerical impact studies on square tubes with tulip triggering (SP2) yielded an unrealistic initial peak load. This may be due to the perfect geometry of triggering tulips. Hence, the effect of initial geometric imperfections on the peak crush load and the corresponding energy absorption is evaluated for square cross sectional composite tube. The results from these analyses are also compared with the experimental results [1].

2. Numerical study

2.1. Case 3– two layers of shell elements with cohesive elements and predefined seams

The details of the experimental impact study, material of the tubes, nomenclature, geometric details, material properties, used damage criteria and the corresponding modelling details are given in Part I.

2.1.1. Modelling with seams

As discussed in the Introduction, due to the absence of axial cracks the failure patterns of the tubes were different from the experimental results. During the experimental crushing of a composite tube, the inner and outer petals were subjected to bending inside and outside of the tube followed by circumferential delamination. The material splaying outwards flared into petals due to the phenomena of axial cracks, and the material splaying inwards showed progressive folding without any petalling [1,9,18]. As a result, a considerable amount of energy was dissipated due to the axial cracking of the outer petals and significant deceleration of the impactor was provided by the inner plies.

2.1.2. Seams

In order to simulate the axial cracks in the outer plies during the crushing process, the seams were introduced at pre-defined location in the outer shell layer of the composite tubes. A seam on the outer shell layer of the composite tube model defines an edge parallel to the axis of the tube that is originally closed; however, it can open during the analysis. These edges are free to move apart. During meshing, duplicate overlapping nodes are placed on the seam; these coincident nodes are free to move apart as the seam separates. Eventually, a seam pre-defines the surface along which the crack has to propagate. Creating duplicate nodes offers several advantages for fracture mechanics calculations. Using this approach, contour integral analysis and crack propagation analysis can be performed [19,20]. However, this work does not deal with

the details of those analyses. A preliminary study on a composite tube using these seams showed that the peak crush load was affected by the introduction of seams. This was obvious, because the peak crush load of a composite tube with seams should be lower than the perfect composite tube. Hence, it is worth investigating the effect of the number of pre-defined seams on the peak crush load of the composite tubes.

During the experimental testing it was observed that the length of the axial cracks on the tubes was equivalent to the total length of deformation of composite tubes [1]. However, before experimental testing the total deformation length of a composite tube for a particular initial impact velocity is unknown. Thus, the seams were introduced approximately for a length of 70 mm at the outer layer of the shell elements. Furthermore, the number of axial cracks differed for each CP tube series for the same impact velocity. Hence, the number of seams is varied from minimum 4 to a maximum of 16 for CP tube series. However, in the case of the SP tube series, during the experimental testing the axial cracks were formed only at the four corners of the tube due to the non-uniform geometry [1]. Hence, for SP1 and SP2 tubes, the number of seams was restricted to 4 at the corners. As explained in Part I, for CP1 tube, the Model D yielded a smaller peak crushing load than Model C. Hence, the approach of the introduction of a pre-defined seam was carried out only for Model D for both CP1 and SP1 tubes.

2.1.3. Results

2.1.3.1. CP1 and SP1 tube series – triggering type 1. The deformation pattern of CP1 tube with 16 seams on the outer shell layer (Fig. 1(a)) provided clear evidence for

the circumferential delamination which split the outer and inner plies. Consequently, axial cracks were formed along the axis of the tubes due to the predefined seams followed by the bending of inner and outer plies. The progressive folding of the inner layer towards the axis of the tube can be clearly noted from Fig. 1(a). Unlike the experimental results, numerical results showed the complete splitting of outer layers at initial time steps. In the case of circular tubes with triggering type 1 (CP1) and type 2 (CP2), there was no significant difference in the failure pattern noticed for the same number of seams. Although the cohesive and seam element approach provided good results for the failure pattern, the predicted peak loads of both tube series CP1 and SP1 were higher than the experimental results due to inadequate triggering modelling (Fig. 2(a) and (b)). On the contrary, the total length of deformation was less than the experimental results (98 and 70 mm against the experimental values 122 and 82.5 mm for CP1 and SP1 tubes respectively). The comparison between the numerical and experimental results is given in Table 1.

2.1.3.2. CP2 and SP2 tube series – triggering type 2. The delamination for CP2 and SP2 took place at the mid thickness of the tube due to the cohesive elements, the inner plies bent towards the centre line of the tube and outer plies bent towards the outside of tube. As an example, the deformation patterns of SP2 are given in Fig. 1(b). There was good correlation of peak crushing load and deformation length observed for CP2 tube (Fig. 3(a)). The numerical peak crushing load of SP2 was comparable with the experimental data, however, the slope of the curve to reach the peak crushing load was higher than the experimental data (Fig. 3(b)). The initial peak crushing load corresponds to the phase at which the delamination takes place at the

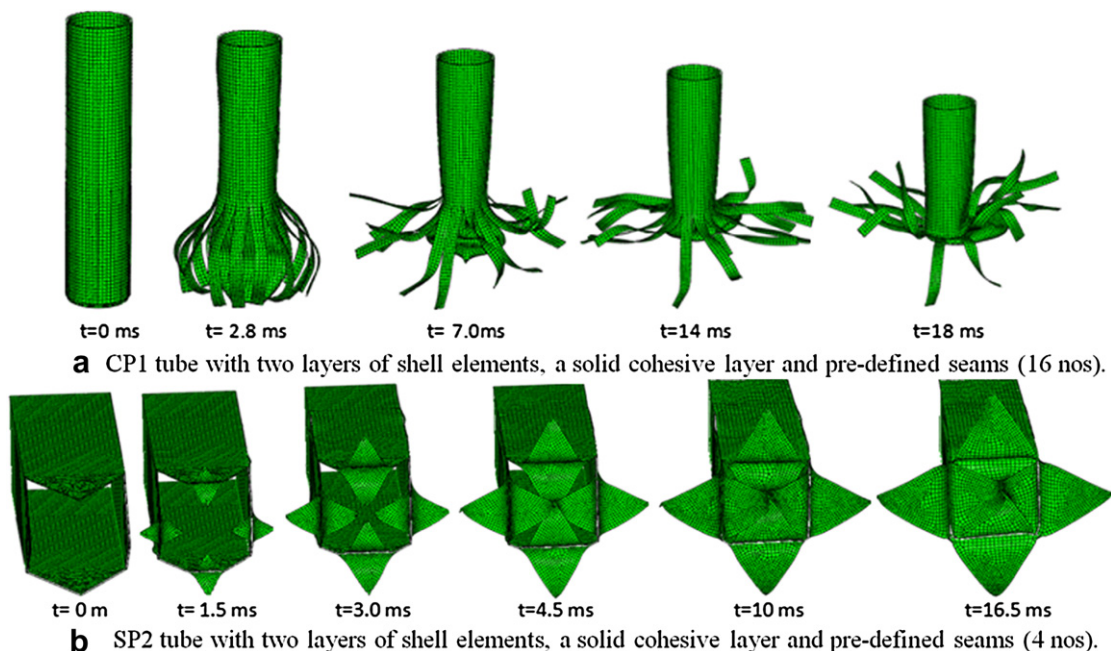


Fig. 1. Deformation sequence of CP1 and SP2 tubes with two layers of shell elements, a solid cohesive layer and pre-defined seams.

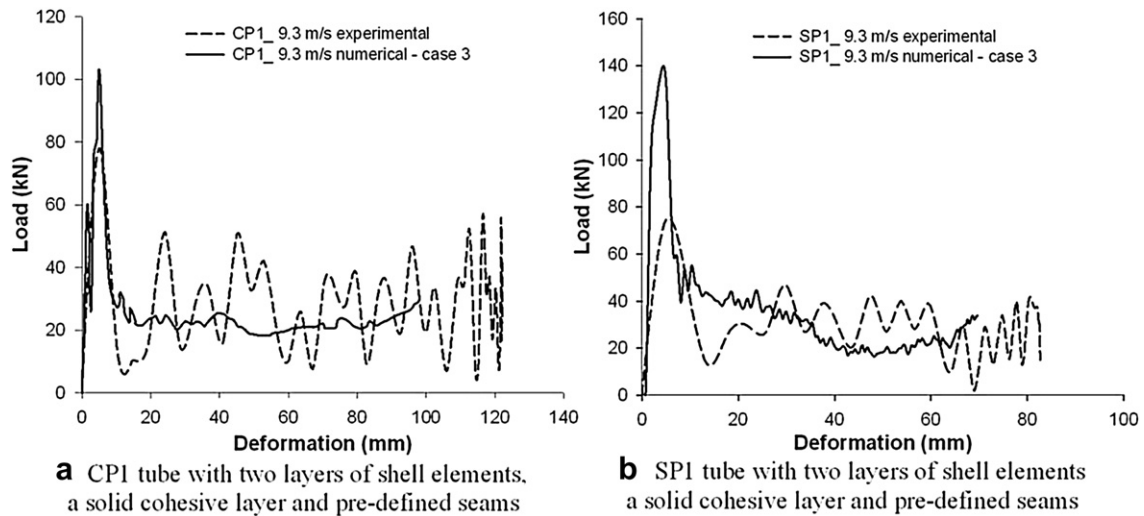


Fig. 2. Comparison of load-deformation curve of CP1 and SP1 tubes with two layers of shell elements, a solid cohesive layer and pre-defined seams.

edges of the tulips. This can be noted from Fig. 1(b) for SP2 tube. Although the peak crush load of SP2 tube was comparable with experimental values, the magnitude of the initial peak was very high. This may be due to the perfect geometric shape of tulips and the corresponding mesh pattern of the square tube. Further study on this phenomenon can be found in section 3.0. The mean crushing loads of tube series CP1, CP2 and SP2 were less than the experimental values. The higher peak crushing load of SP1 was attributed to a higher mean crush load (refer Table 1 for corresponding energy absorption values).

2.2. Case 4 - Multiple layers of shell elements with cohesive elements and without seams

2.2.1. Modelling

The predicted higher peak crushing load from Case 3 indicated that the numerical modelling of triggering, particularly for type 1, was insufficient to capture the accurate peak crush load. Moreover, during the experimental test, in addition to the major circumferential delamination at the mid-thickness of the tube, multiple delaminations were observed in all sub-laminates during the bending of plies. This phenomenon significantly altered the bending stiffness of the plies [1,7,18]. Hence, the numerical modelling of multiple delaminations is absolutely necessary to account for the energy dissipation in each ply, which significantly contributes to the peak and

mean crushing loads of a composite tube. In order to isolate the effect of multiple delaminations on the energy absorption and deformation pattern, the thickness of the composite tubes was modelled with six layers of shell elements without seams. Accordingly, the thickness of each shell layer was divided equally. Five layers of solid cohesive elements were placed in between the shell elements. The length of the inner most shell layer was 220 mm and the length of outer shells and cohesive layers were chosen to form 45° edge chamfering. It can be noted from the schematic representation (Fig. 4) that the multiple layers of shell elements formed the correct geometry of the composite tube for triggering type 1.

2.2.2. Results

2.2.2.1. CP1 and SP1 tube series – triggering type 1. Due to the larger number of elements, the computation time was much larger than the previous cases. The deformation sequence of CP1 and SP1 tubes was very similar to Case 2 of Part I (initial progressive crushing at triggering location followed by local buckling). The numerical peak crushing load of the tube series CP1 was very close to the experimental results (Fig. 5(a)). However, in the case of SP1 tube series there was a higher peak force (refer Fig. 5(b)). The comparative study of the average crushing load and the energy absorption is given in Table 1. For the CP1 tube, the maximum deformation length of 120 mm was noted

Table 1

Comparison of experimental and numerical simulation results.

Cases	Peak crush load (kN) P_{max}				Mean crush load (kN) P_{avg}				Deformation length (mm) l_{max}				Absorbed energy (kJ) E_d			
	CP1	CP2	SP1	SP2	CP1	CP2	SP1	SP2	CP1	CP2	SP1	SP2	CP1	CP2	SP1	SP2
Experimental [1]	78	69	73	73	28.3	26.0	31.1	37.7	122	133	82.5	71	3.462	3.47	2.563	2.68
Numerical Case 3	103	67	139	81	24.6	19.0	35.9	25.5	98	125	70	90	2.41	2.30	2.513	2.30
Numerical Case 4	75	72	100	92	20.5	23.5	26.5	26.5	120	127	93	94	2.45	3.00	2.464	2.50
Numerical Case 5	82	64	95	69	25.7	24.3	43.3	24.9	130	140	70	98	3.34	3.40	3.033	2.46

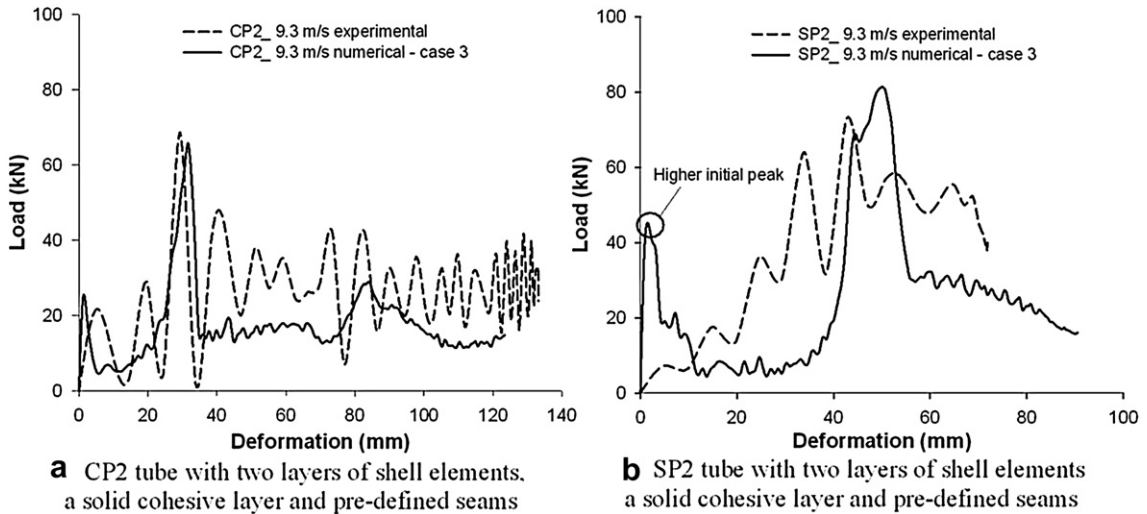


Fig. 3. Comparison of load-deformation curve of CP2 and SP2 tubes with two layers of shell elements, a solid cohesive layer and pre-defined seams.

against the experimental value of 122 mm. In contrast to the CP1 tube, the SP1 tube exhibited higher deformation length (94 mm) than the experimental value (82.5 mm).

2.2.2.2. CP2 and SP2 tube series – triggering type 2. Although the approach of Case 2 in Part I captured the comparable peak crush load with the experimental results for triggering type 2 series, the deformation lengths of these types were not well correlated with the experimental data. Hence, a numerical investigation was carried out with the multiple layers approach. The deformation pattern of CP2 and SP2 tube series was very similar to the Case 2 of Part I (delamination between plies and progressive crushing without axial cracks). In the case of CP2 tube, there was good correlation observed between the experimental and numerical results for the peak crushing load and the total deformation length (Fig. 6(a)). However, the numerical

peak crushing load and the total deformation length of SP2 were higher than the experimental values (Fig. 6(b)). Furthermore, the slope to reach the peak load was higher compared to the experimental data. This may be due to the reduced stiffness offered by the outer shell layers at the initial time increments. Similar to Case 3, there was an initial peak observed before reaching the peak crush load. This phenomenon is explained in section 3.0 which deals with initial geometric imperfections.

2.3. Case 5– multiple layers of shell elements with cohesive elements and seams

2.3.1. Modelling

In order to achieve the correct peak crush load (especially for triggering type 1) with multiple delaminations and to achieve the typical failure patterns of the composite

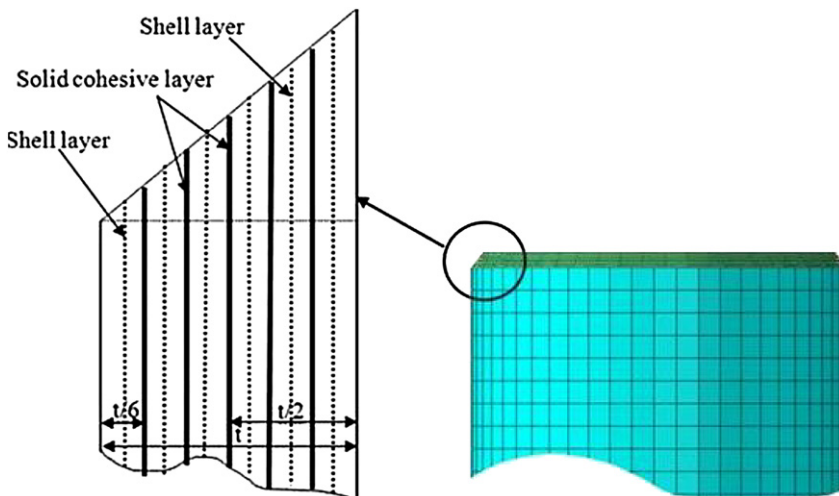


Fig. 4. Finite element modelling of CP1 tube series with multiple layers of shell elements and solid cohesive layers.

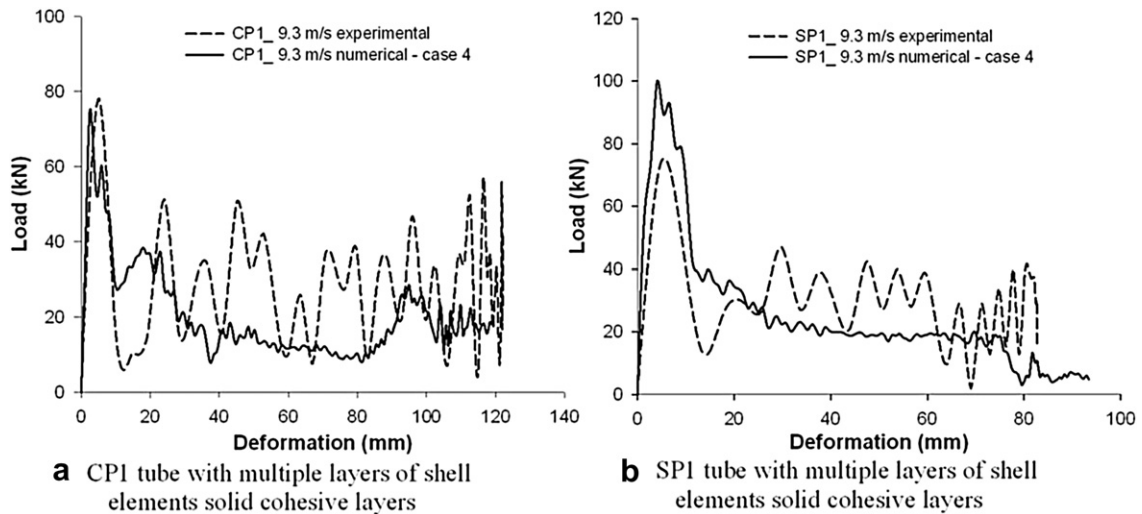


Fig. 5. Comparison of load-deformation curve of CP1 and SP1 tubes with multiple layers of shell elements and solid cohesive layers.

tubes, the approach of multiple layers of shell elements with the combination of cohesive elements and seams was investigated. The number of shell layers (six) was divided in half and the seams were assigned only to the outer shell layers.

2.3.2. Results

2.3.2.1. CP1 and SP1 tube series – triggering type 1. The deformation patterns of the CP1 tubes with 16 seams are shown in Fig. 7(a). Due to the predefined seams, the results of the initial time increments showed complete splitting of the outer shell layers at the assigned locations of seams, while the inner plies continued to fold inside. The later stages of the analysis gave clear evidence of the bending of elements which belong to the outer shell layers. The numerical modelling approach with multiple layers of shell

elements with cohesive elements and seams showed very good correlation of the deformation patterns with the experimental results. The effect of the number of predefined seams on the peak load was studied for CP1 tube. Two analyses were carried out with 8 and 16 seams for an impact velocity of 9.3 m/s. The corresponding force versus deformation histories of these two cases are presented in Fig. 8(a). There was no significant difference in the magnitude of peak crush load observed between these two cases. However, after 40 mm deformation length, a considerable difference in the mean load reduction was observed. The deformation pattern of SP1 tube at different time intervals is shown in Fig. 7(b). Similar to CP1 tube, the SP1 tube also exhibited multiple delaminations. The subsequent stages of SP1 tube showed that the inner plies were subjected to compression rather than uniform progressive folding. As a result, the crushing force was

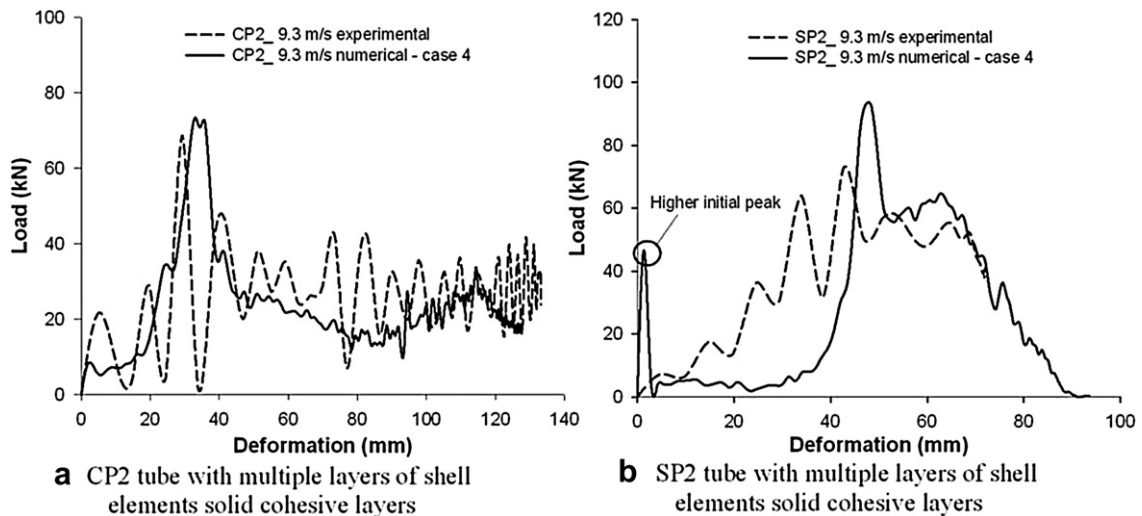


Fig. 6. Comparison of force-deformation curve of CP2 and SP2 tubes with multiple layers of shell elements and solid cohesive layers.

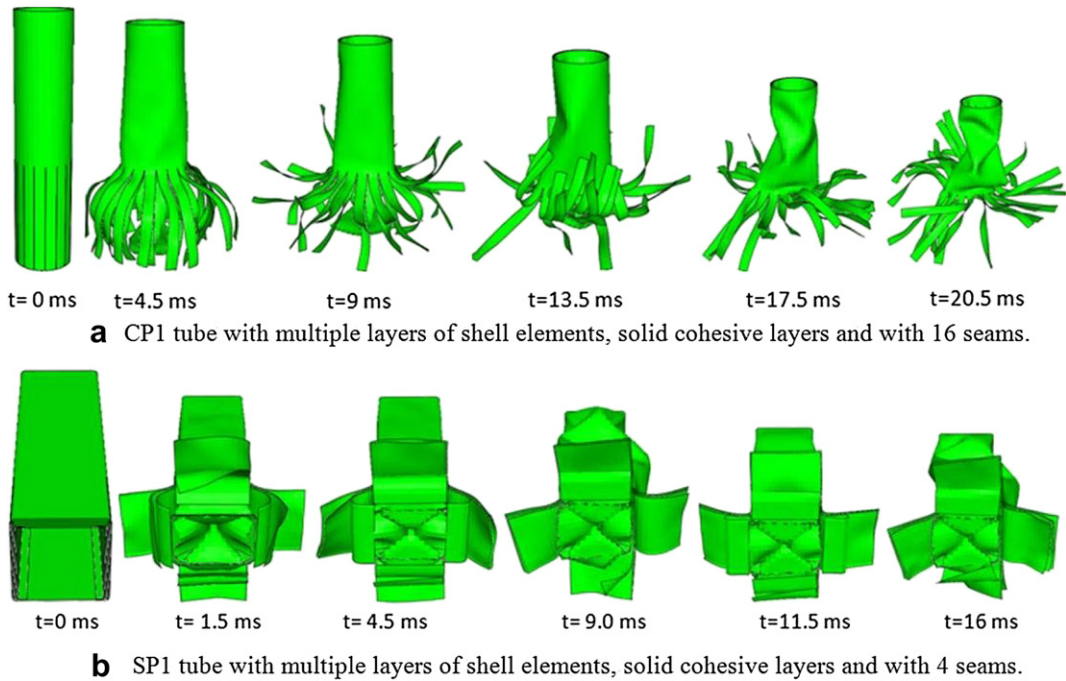


Fig. 7. Deformation sequence of CP1 and SP1 tubes with multiple layers of shell elements, solid cohesive layers and pre-defined seams.

increased considerably after attaining 50 mm of deformation length (Fig. 8(b)). Consequently, the total deformation length of the tube was lower compared to the Case 4 (70 mm against 93 mm).

2.3.2.2. CP2 and SP2 tube series – triggering type 2. The experimental deformation pattern of the circular tubes (CP1 and CP2) yielded more than 10 major axial cracks along the axis of the tube. The effect of the number of seams on the peak crush load was studied with CP1 tube. To understand the deformation sequence in detail, the CP2

tube was modelled only with 4 seams. The results of the numerical analysis at different time intervals are shown in Fig. 9(a). The initial stages of CP2 showed clear evidence of the delaminations between all the shell layers. Consequently, the outer plies were subjected to outside bending and the inner materials bent inwards. This phenomenon can be well observed from Fig. 9(a). The correlation of the experimental and the numerical results is shown in Fig. 10 (a). Similarly, the deformation pattern of SP2 tube at different time intervals showed clear indication of all typical failure modes of a brittle composite tube (Fig. 9(b)).

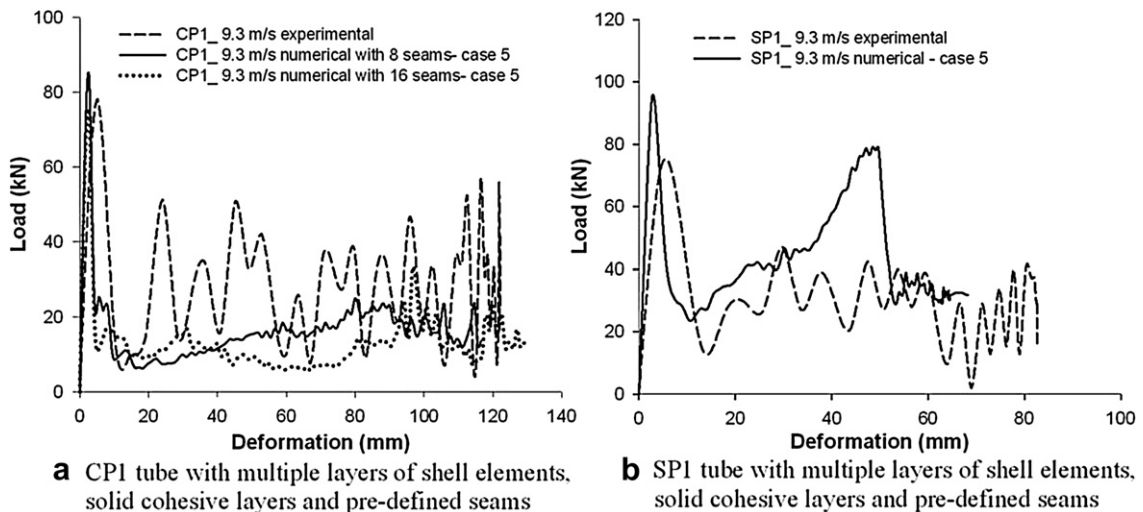


Fig. 8. Comparison of load-deformation curve of CP1 and SP1 tubes with multiple layers of shell elements, solid cohesive layers and with pre-defined seams.

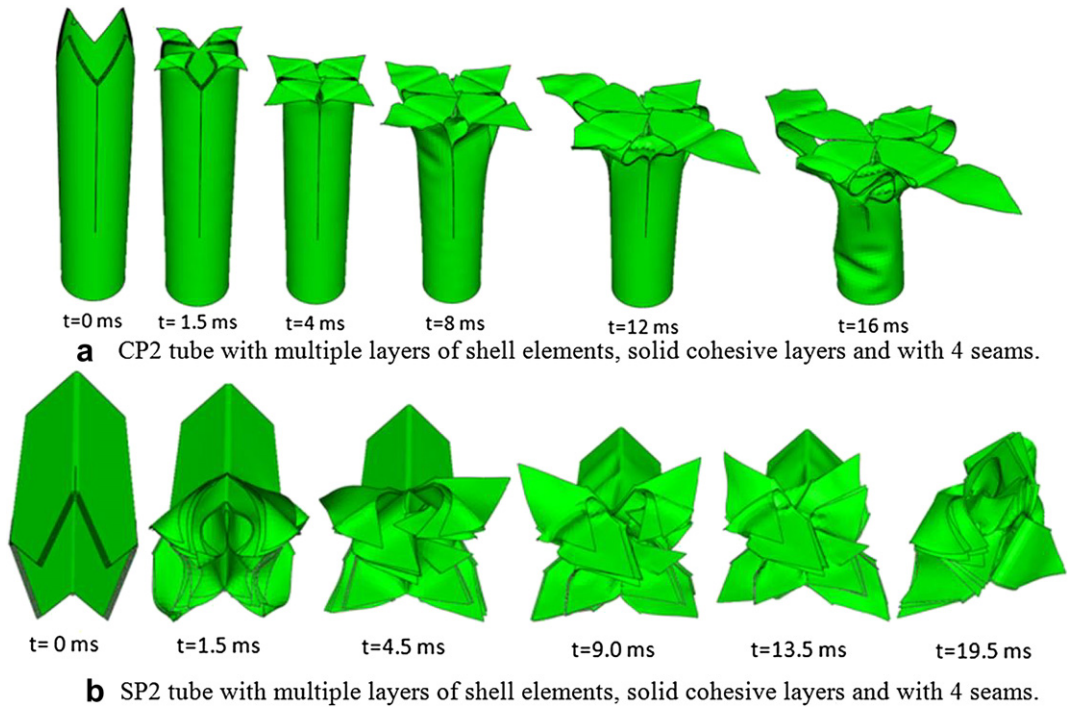


Fig. 9. Deformation sequence of CP2 and SP2 tubes with multiple layers of shell elements, solid cohesive layers and with pre-defined seams.

As discussed earlier, the number of seams for SP2 tube was restricted to only 4 at the corners of the tube. For SP2, similar to Cases 3 and 4, a delay in the peak crushing load and an initial peak crush load were observed (Fig. 10(b)).

2.4. Discussion of results

2.4.1. Comparison of deformation patterns

From the above numerical parametric study, the approach from Case 3 and Case 5 provided good correlation of the deformation patterns for the circular and square

composite tubes. Hence, in this section a comparison of the failure patterns of these cases are discussed with the experimental results [1]. As discussed, from Case 3 and 5 there was no significant difference in the deformation pattern noted between CP1 and CP2 tube series. So, the failure patterns of tube series CP1, SP1 and SP2 only are taken into consideration. The experimental failure pattern of these three tube series for the impact velocity of 9.3 m/s are again reproduced in Fig. 11(a). Similarly, the deformation patterns of two layers (Case 3) and multiple layers (Case 5) of shell elements with cohesive elements and

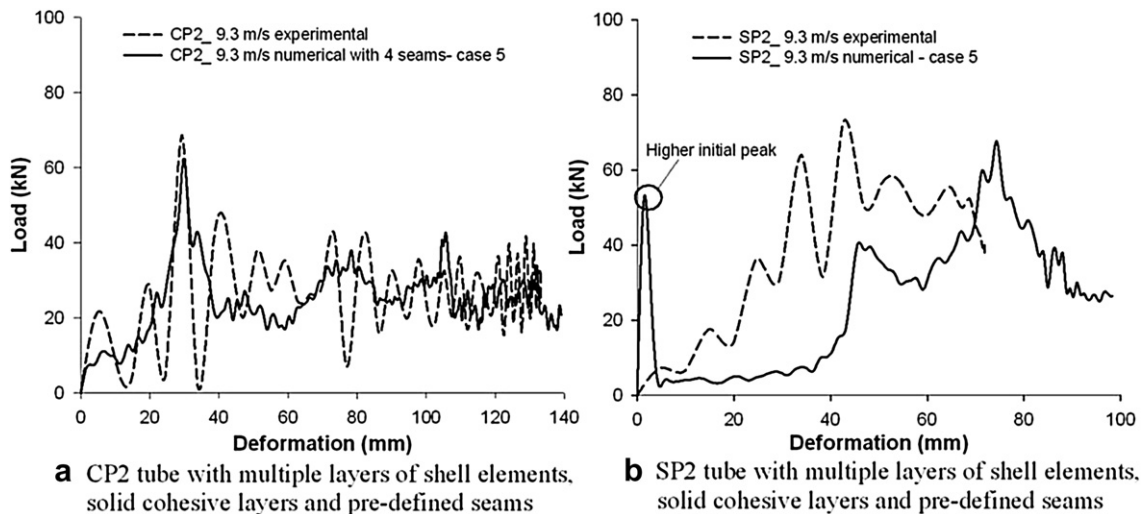


Fig. 10. Comparison of load-deformation curve of CP2 and SP2 tubes with multiple layers of shell elements, solid cohesive layers and with pre-defined seams.

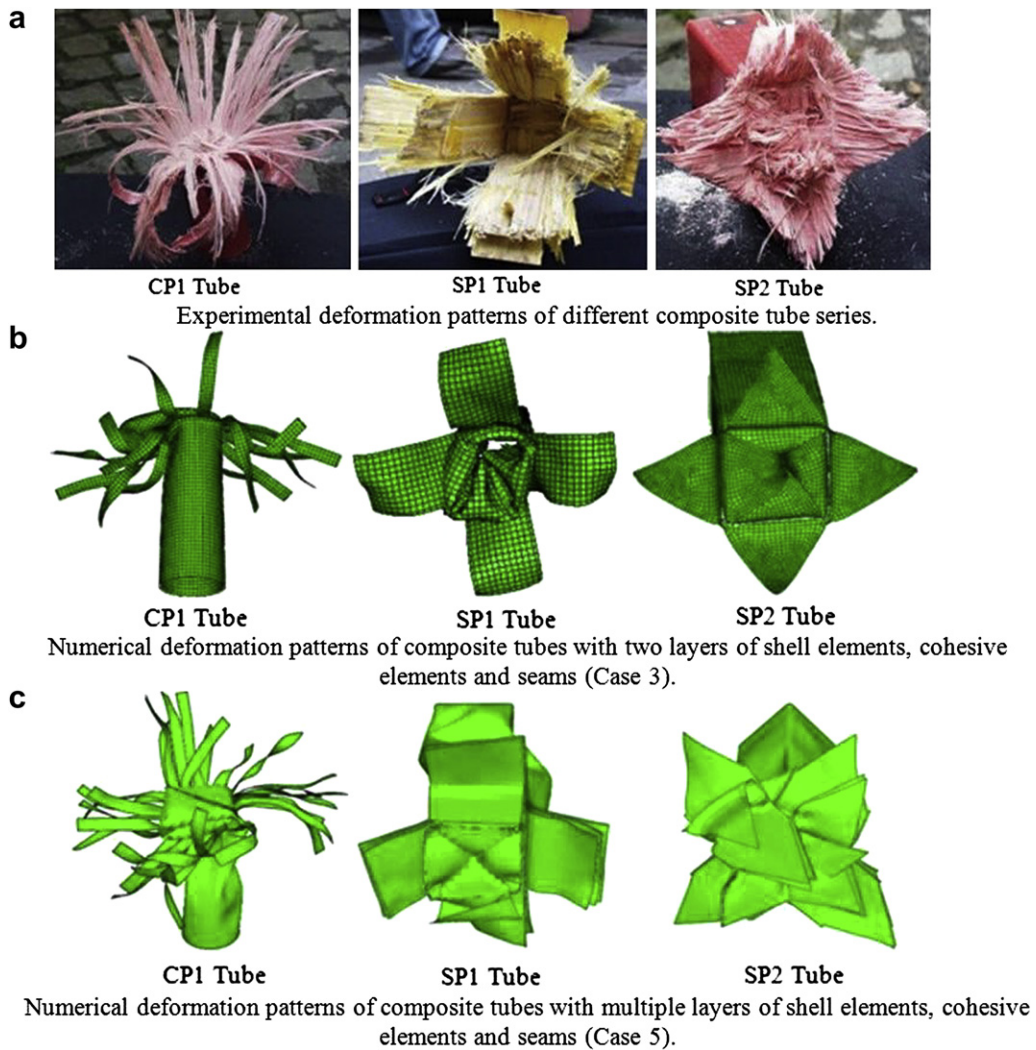


Fig. 11. Comparison of experimental and numerical deformation patterns.

seams are shown in Fig. 11(b) and (c) respectively. The approach of Case 3 showed clear evidence of all the macro failure mechanisms of the circular and square composite tubes. However, this approach cannot capture the multiple delaminations which occur at the time of failure of a composite tube. The approach with the multiple layers of shells with cohesive elements and seams provided very good correlation of failure patterns in all cases of tube series. Similar to the Case 3 approach, from Case 5 all the failure modes (delamination, axial cracks, bending of petals and fracturing) of a brittle composite tube are clearly evident.

2.4.2. Comparison of crush loads and energy absorption

The comparison of the peak crush load (P_{max}), mean crush load (P_{mean}), deformation length (l_{max}) and the corresponding energy absorption (E_d) of the experimental data [1] and different approaches of the numerical simulation are given in Table 1. For triggering type 1 series (CP1 and SP1), the Case 3 approach yielded lower peak loads than the

Case 2 which was discussed in Part I. However, the predicted peak loads of this approach were higher than the experimental values. This gives a clear indication that the modelling of triggering with two layers of shell elements and cohesive elements was inadequate to capture the right peak crush load. Due to this effect, the predicted deformation length and the corresponding energy absorption of the tube series (CP1, CP2 and SP1) were smaller than the experimental data. The peak loads from the multiple delaminations approach (Cases 4 and 5) provided closer values for all tube series compared to experimental data. This clearly indicates that the multiple delaminations have to be considered for the energy absorption calculations of composite tubes. The peak loads of SP1 tube series for these two approaches were lower than other approaches; however, the predicted peak loads were higher than the experimental values. The multiple layers of shell elements approach (Cases 4 and 5) provided a better energy absorption values compared to two layers of shell elements. The Case 5 (multiple layers with cohesive elements and

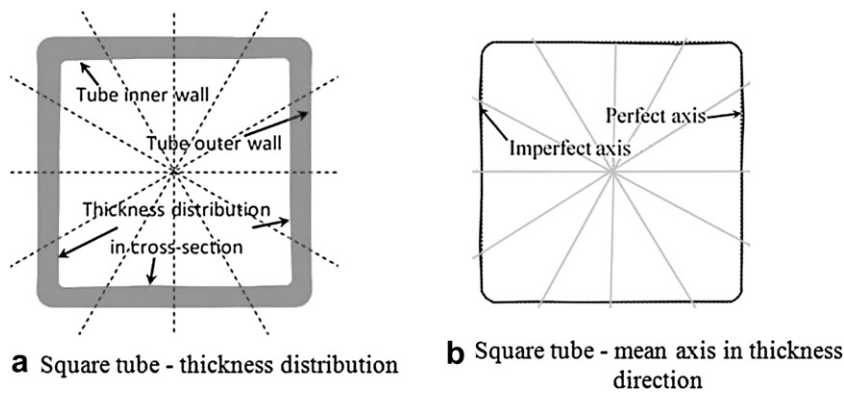


Fig. 12. Typical measured cross sectional polar diagram of square composite tube.

pre-defined seams) approach predicted a much closer values of energy absorption than any other approach, which can be noted from the Table 1.

3. Effect of initial geometric imperfections

The numerical impact studies (Cases 1 to 5) on square tubes with tulip triggering (SP2) yielded an unrealistic initial peak load. This may be due to the perfect geometry of triggering tulips and the corresponding mesh patterns. In order to evaluate the effect of geometry imperfection on this initial peak load and the corresponding crushing performance, a study was conducted with initial geometric imperfections. A representative composite specimen from SP2 series was taken for the study, and the initial geometric imperfections of the tube was measured and recorded. The investigation of outer and inner surfaces of the tested composite tube specimen showed good evidence of similar geometric imperfections throughout their length (220 mm). The outer width and the thickness were measured at regular intervals along radial and

longitudinal directions of the tube. The inner surface measurement was used to determine the initial imperfections on the shell wall distribution. The difference between the outer and inner surface measurements was considered as a composite shell thickness distribution. The average measured thickness of SP2 tube was 4.554 mm (nominal thickness is 4.5 mm). Fig. 12(a) shows the typical polar diagram of measured cross section of square (SP2) composite tube. Furthermore, Fig. 12(b) shows deviation of the tube from the perfect square section. The corresponding experimental result of this composite tube was taken into consideration for the comparison of results. As discussed in Part I, the delamination phenomenon cannot be captured with the single layer of shell elements approach. Hence, the study of the effect of initial geometric imperfections with the single layer of shell elements is not considered. The effect of geometric imperfections is studied for the Cases 2 to 5. The modelling approaches of these cases (Cases 2 to 5) with geometric imperfections are similar to the perfect tube geometry analyses.

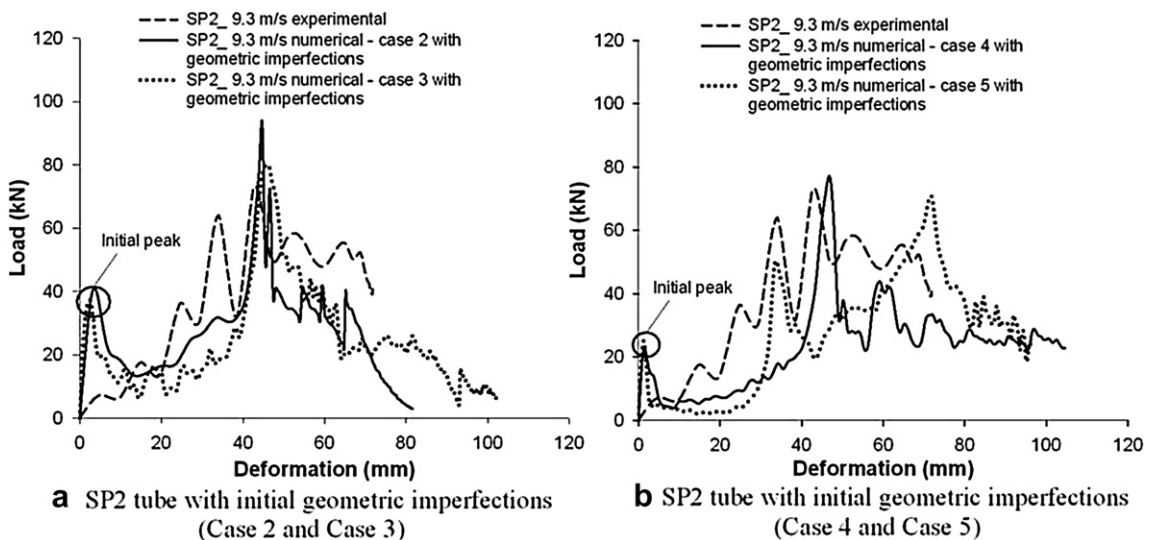


Fig. 13. Comparison of load - deformation histories of SP2 tube with initial geometric imperfections.

Table 2

Summary of numerical impact parameters for SP2 tube with measured initial geometric imperfections.

Cases	Peak crush load (kN) P_{max}	Mean crush load (kN) P_{avg}	Deformation length (mm) l_{max}	Absorbed energy (kJ) E_d
Square glass polyester tube with triggering type 2 (SP2)				
Experimental [1]	73	37.7	71	2.68
Numerical study with the measured initial geometric imperfections				
Case 2 with geometric imperfections	93.0	25.8	82.5	2.13
Case 3 with geometric imperfections	79.9	23.4	102	2.39
Case 4 with geometric imperfections	76.8	23.5	104	2.44
Case 5 with geometric imperfections	70.5	25.2	94	2.50

3.1. Results and discussion

The results of the numerical analyses (Cases 2 to 5) of SP2 tube with measured initial geometric imperfections are presented in Fig. 13. The results from these numerical analyses showed no significant difference in the deformation pattern compared to the perfect geometry analyses. However, there was a distinctive difference in the initial peak load noted. It can be seen from Fig. 13 that the magnitude of initial peak decreased compared to perfect tube geometry analyses. For Case 2 (two layers of shell elements), the magnitude of the initial peak load 60 kN (case without imperfection) was reduced to 40 kN (case with imperfection). Furthermore, this magnitude is reduced to 36 kN for Case 3 with geometric imperfection. An important conclusion can be made from Fig. 13 that the magnitude of the initial peak crush load was considerably reduced as the number of shell element layers (with initial geometry imperfection) increased. For Cases 4 and 5 the initial peak magnitude was further reduced to approximately 20 kN. The approach of two layers of shell elements with geometric imperfections provided no significant difference in the peak crush load. However, Cases 4 and 5 showed a distinct difference in the peak crush load compared to perfect tube analyses (Fig. 13)(b). However, the mean crush load of these cases was very close to the without imperfection cases. As a result, the calculated energy for the cases with and without imperfections is comparable (Tables 1 and 2).

4. Conclusions

This paper focused on the importance of considering multiple delaminations to predict the correct energy absorption of the brittle composite tubes. In order to study this effect in detail, a comprehensive numerical simulation was conducted for both circular and square cross sectional pultruded profiles made of glass-polyester with two triggering mechanisms. The effect of multiple delaminations on the peak crushing load, deformation length and the corresponding energy absorption was proved by comparison with experimental data. Furthermore, this paper demonstrated the effect of modelling issues of triggering geometry, especially the triggering type 1 (45° edge chamfering). Both the above factors were demonstrated with multiple layers of shell elements and cohesive elements. The concept of pre-defined seams was successfully

employed to simulate the correct deformation patterns of circular and square cross section composite tubes. Using this approach, there was very good correlation observed between the numerical and experimental deformation patterns. The typical failure modes of brittle composite tubes, such as central delamination, bending of inner and outer plies, axial cracks and fibre fracturing are clearly evident from the numerical deformation patterns. The effect of the number of pre-defined seams on the peak crush load and the corresponding energy absorption was evaluated. Furthermore, the effect of initial geometric imperfections on the crushing performance of the composite tube was also presented. From the result of the numerical simulation it can be concluded that:

- To capture multiple delaminations and to model the correct geometry of the triggering type 1, the approach of multiple layers of shell elements is absolutely necessary (Cases 4 and 5). Both these approaches provided peak crush loads which were closer to the experimental values for the tube series CP1, CP2, SP2. However, the deformation pattern obtained from the former approach (Case 4) was similar to Case 2 of Part I.
- The implementation of seams (to generate axial cracks) for the Cases 3 and 5 provided very good evidence of all macroscopic and microscopic deformation mechanisms of pultruded circular and square composite tubes. The corresponding energy absorption values were very close to the experimental values.
- The different approaches with initial geometric imperfection analyses of square cross sectional composite tube showed no significant change in the deformation patterns compared to perfect tube geometry analyses. There was a difference in peak crush load noted. However, the effect of change in the peak crush load on the total energy absorption is negligible. Furthermore, the perfect geometry of the tulips and the number of shell layers have a large influence on the initial peak load. Introduction of initial geometric imperfection and increasing the number of shell layers can help to achieve a realistic initial peak load.

Acknowledgements

The authors gratefully acknowledge the financial support of the “Fund for Scientific Research” – Flanders (F.W.O) (Grant No: G.0114.07).

References

- [1] S. Palanivelu, W. Van Paepegem, J. Degrieck, J. Van Ackeren, D. Kakogiannis, D. Van Hemelrijck, J. Wastiels, J. Vantomme, Experimental study on the axial crushing behaviour of pultruded composite tubes, *Polymer Testing* 29 (2) (2010) 224–234.
- [2] R.C. Batra, N.M. Hassan, Blast resistance of unidirectional fiber reinforced composites, *Composites Part B: Engineering* 39 (3) (2008) 513–536.
- [3] A.G. Mamalis, D.E. Manolacos, M.B. Ioannidis, P.K. Kostazos, Crushing of hybrid square sandwich composite vehicle hollow bodysHELLS with reinforced core subjected to axial loading: numerical simulation, *Composite Structures* 61 (3) (2003) 175–186.
- [4] C. Mcgregor, R. Vaziri, X. Xiao, Finite element modelling of the progressive crushing of braided composite tubes under axial impact, *International Journal of Impact Engineering* 37 (6) (2010) 662–672.
- [5] H. Zarei, M. Kröger, H. Albertsen, An experimental and numerical crashworthiness investigation of thermoplastic composite crash boxes, *Composite Structures* 85 (3) (2008) 245–257.
- [6] H. Suemasu, W. Sasaki, T. Ishikawa, Y. Aoki, A numerical study on compressive behavior of composite plates with multiple circular delaminations considering delamination propagation, *Composites Science and Technology* 68 (12) (2008) 2562–2567.
- [7] X.W. Wang, I. Pont-Lezica, J.M. Harris, F.J. Guild, M.J. Pavier, Compressive failure of composite laminates containing multiple delaminations, *Composites Science and Technology* 65 (2) (2005) 191–200.
- [8] A.F. Johnson, M. Holzapfel, Influence of delamination on impact damage in composite structures, *Composites Science and Technology* 66 (6) (2006) 807–815.
- [9] S. Palanivelu, R. Verhelst, W. Van Paepegem, J. Degrieck, D. Kakogiannis, D. Van Hemelrijck, J. Wastiels, K. De Wolf, J. Vantomme, Experimental and numerical study on axial crushing behaviour of pultruded composite tubes, *Proceeding of the 13th European conference on composite materials, Stockholm, Sweden; June 2–5, 2008*.
- [10] J. Oh, M. Cho, J.-S. Kim, Buckling analysis of a composite shell with multiple delaminations based on a higher order zig-zag theory, *Finite Elements in Analysis and Design* 44 (11) (2008) 675–685.
- [11] S. Li, S.R. Reid, Z. Zou, Modelling damage of multiple delaminations and transverse matrix cracking in laminated composites due to low velocity lateral impact, *Composites Science and Technology* 66 (6) (2006) 827–836.
- [12] M.W. Hilburger, J.H. Starnes, Effects of imperfections of the buckling response of composite shells, *Thin-Walled Structures* 42 (3) (2004) 369–397.
- [13] J. Arbocz, J.M.A.M. Hol, Collapse of axially compressed cylindrical shells with random imperfections, *Thin-Walled Structures* 23 (1–4) (1995) 131–158.
- [14] W. Koiter, On the stability of elastic equilibrium, Ph.D. Thesis., Polytechnic Institute Delft, English Translation: NASA TT F-10, 1945 (1967) 833.
- [15] M.K. Chryssanthopoulos, V. Giavotto, C. Poggi, Characterization of manufacturing effects for buckling-sensitive composite cylinders, *Composites Manufacturing* 6 (2) (1995) 93–101.
- [16] J.B.C. Arbocz, The effect of general imperfections on the buckling of cylindrical shells, *Journal of Applied Mechanics* 36 (Series E(1)) (1969) 28–38.
- [17] C. Bisagni, Numerical analysis and experimental correlation of composite shell buckling and post-buckling, *Composites Part B: Engineering* 31 (8) (2000) 655–667.
- [18] S. Palanivelu, W. Van Paepegem, J. Degrieck, D. Kakogiannis, J. Van Ackeren, D. Van Hemelrijck, J. Wastiels, J. Vantomme, Comparative study of the quasi-static energy absorption of small-scale composite tubes with different geometrical shapes for use in sacrificial cladding structures, *Polymer Testing* 29 (3) (2010) 381–396.
- [19] ABAQUS Theory Manual. ABAQUS, Inc. and Dassault Systèmes, 2007.
- [20] ABAQUS User Manual. ABAQUS, Inc. and Dassault Systèmes, 2007.